

CURRENT DENSITY AND WAVE POLARIZATION OBSERVED IN DENSITY HOLES UPSTREAM OF EARTH'S BOW SHOCK

G. Parks^a, E. Lee^a, N. Lin^a, A. Teste^a, M. Wilber^a, I. Dandouras^b, H. Réme^b
and M. Goldstein^c

^a*Space Sciences Laboratory, UC Berkeley, Berkeley, CA*

^b*C. E. S. R., Toulouse, France.*

^c*NASA GSFC, Greenbelt, MD*

Abstract. Previous articles [1,2] have shown density holes are regions of density depletions below the solar wind level with scale length of an ion gyroradius. Density holes have steepened edges seen in both particles and fields. Here we present first observations of currents and wave polarizations associated with density holes. We show an example of current density determined from four point Cluster observations that has a value ~ 150 nA m⁻². The waves are elliptically polarized and rotating in the sense of ions (left hand) in the plasma frame. The significance of these observations are still being studied. The waves appear to grow and steepen as the density holes are convected with the solar wind toward the Earth. The transient nature of density holes suggests that the temporal features could represent the different stages of nonlinear evolutionary processes that produce a shock-like structure.

Keywords: density holes, foreshock cavities, hot flow anomalies.

PACS: 93.30.Qd, 96.50 Tf, 96.60 Vg

INTRODUCTION

The Earth's bow shock is the best-studied example of a collisionless shock discontinuity in space. Although much is known about the bow shock, fundamental questions still remain unanswered. It is still not known what physics can produce a shock-like discontinuity in collisionless plasmas. Clues to this fundamental problem have been recently obtained from observing the behavior of "density holes" upstream of Earth's bow shock [1, 2].

Density holes are the smallest known nonlinear ion structures observed in the upstream region of the bow shock. Density holes have dimensions on the order of an ion Larmor radius. While they resemble previously studied upstream structures, hot flow anomalies (HFAs) [3], hot diamagnetic cavities (HDCs) [4] and foreshock cavities (FCs) [5], density holes are shorter in duration and have deeper holes. Density

holes also occur much more frequently than HFAs and HDCs that have been observed only rarely. Density holes have large flow deviations similar as in HFAs and HDCs. Foreshock cavities have overshoots in density and magnetic field intensities at their edges but they do not have the strong density depletions that define density holes. Density holes are observed under a variety of solar wind conditions but only in the presence of back streaming bow shock particles. However, not all back streaming particles produce density holes. The mechanisms that can produce density holes still remain unknown. In this article we will further characterize observational properties of density holes, by presenting first results of currents and wave polarization of typical density holes. A more detailed study of waves can be found in [6].

Two density holes were observed on 2 April 2002 (Figure 1) by Cluster 1 in front of the bow shock located at a distance of (9.8, -2.2, 8.1) R_E (Geocentric Solar Ecliptic coordinates are used throughout).

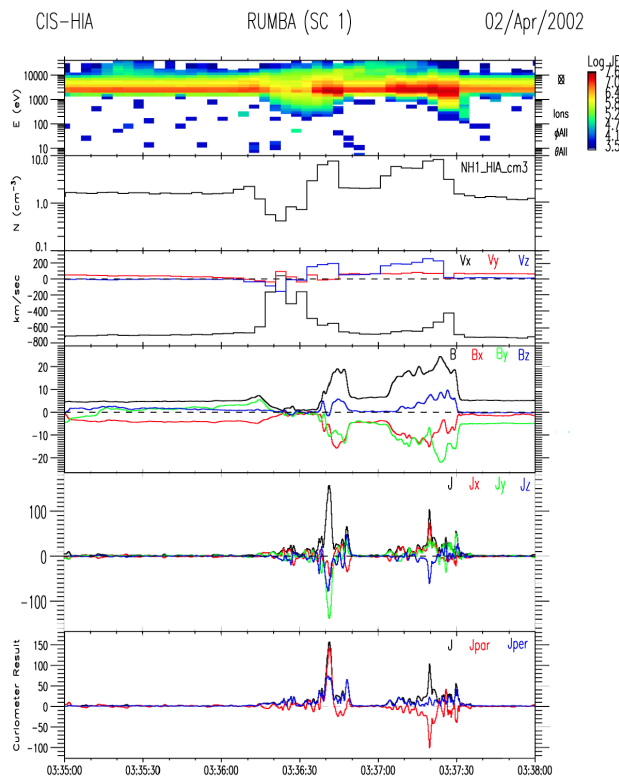


FIGURE 1. Spin averaged (4s) bulk parameters obtained from the distribution function obtained by an ion instrument and magnetometer on Cluster. From top to bottom, energy spectrogram, density, bulk speeds and magnetic field in GSE. The bottom two panels are currents derived from the curlmeter technique using the four spacecraft data.

Let us now focus on the first density hole with the minimum at $\sim 0336:20$ UT. The density in the hole is $\sim 0.4 \text{ cc}^{-1}$, which is a factor of ~ 4 less than the solar wind density,

n_{sw} , $\sim 1.6 \text{ cc}^{-1}$. Both edges show increase of the density but the overshoot is much larger on the upstream edge. The density here is $\sim 8 \text{ cc}^{-1}$ and about five times larger than the n_{sw} . Large solar wind deviation is commonly observed with all density holes. In this particular example, the solar wind V_x $\sim 700 \text{ km s}^{-1}$ was reduced to $\sim 0 \text{ km s}^{-1}$. The density holes are dynamic and the holes are expanding and pressure is not balanced [1]. Note V_z increased from ~ 0 to 200 km s^{-1} at the edge. The temperature in the hole increased to more than $10^7 \text{ }^\circ\text{K}$ (not shown; See examples [1]). The shape of the magnetic field $|\mathbf{B}|$ is very similar to the shape of the density hole with similar overshoot at the edge and hole in the center indicating particles and fields are closely coupled. Note that B_y changed sign across the density hole indicating crossing of a current sheet. Current sheets are associated with most density holes we have studied. Observations of density holes by four Cluster spacecraft separated by a few hundred kilometres allow us to compute the current density (\mathbf{J}) using the ‘‘curlometer’’ technique [7-11]. Current densities in GSE system and relative to the directions of the \mathbf{B} -field are shown in the bottom two panels. The largest $|\mathbf{J}|$ are observed with the overshoot in the upstream edge. The peak $|\mathbf{J}|$ is $\sim 150 \text{ nA m}^{-2}$. Currents are flowing mostly parallel to \mathbf{B} although there are also currents perpendicular to \mathbf{B} . The currents along \mathbf{B} are carried by electrons (not shown).

Figure 2 shows another example of a density hole observed on 3 February 2002. This event has all of the features of the density hole shown in Figure 1. We see deviation of the solar wind flow with $V_x \sim 400 \text{ km s}^{-1}$ reducing to $\sim 100 \text{ km s}^{-1}$, V_y increasing from ~ 0 to 200 km s^{-1} , and V_z from ~ 0 to -400 km s^{-1} , depletion of the density from 10 cc^{-1} to $\sim 1.5 \text{ cc}^{-1}$, increase of the temperature from $T \sim 10^6 \text{ }^\circ\text{K}$ outside the hole to $2 \times 10^7 \text{ }^\circ\text{K}$ in the hole, overshoot of the density at the edges with a much larger one on the upstream side ($\sim 50 \text{ cc}^{-1}$) than the downstream side ($\sim 20 \text{ cc}^{-1}$) and the magnetic field $|\mathbf{B}|$ has similar shape as the density hole.

We have used the high time resolution \mathbf{B} -field (22.5 Hz) and \mathbf{E} -field (25 Hz) measurements to determine the phase velocity and the sense of polarization for this density hole. We assume that the wave front is planar and uniform on the scale of the spacecraft separation (a few hundred kilometers) and that the waves are propagating with a constant phase velocity. Then the phase speed in the plasma frame can be computed from $V_{pl} = V_{ph} - \mathbf{k} \cdot \langle \mathbf{V} \rangle_{sw}$ where V_{pl} is the phase speed in the plasma frame, V_{ph} is the phase speed in the spacecraft frame, \mathbf{k} is the wave normal, and $\langle \mathbf{V} \rangle_{sw}$ is the average bulk speed. The normal \mathbf{k} is determined from minimum (maximum) variance analysis for $\delta \mathbf{B}$ ($\delta \mathbf{E}$). We use Faraday’s law and obtain $\mathbf{k} \times \delta \mathbf{E} = -\omega \delta \mathbf{B}$ where ω is the frequency and $\delta \mathbf{E}$ and $\delta \mathbf{B}$ are fluctuations of \mathbf{E} and \mathbf{B} fields. The phase speed in the spacecraft frame is obtained from $V_{ph} = (\omega/k) = \mathbf{k} \cdot (\delta \mathbf{E} \times \delta \mathbf{B}) / \delta B^2$. Doppler shifting it yields the phase speed in the plasma frame. We will examine low frequency waves close to the ion Larmor frequency that are present with density holes [1,2]. A detailed discussion of the timing method and the wave properties are further given in [6].

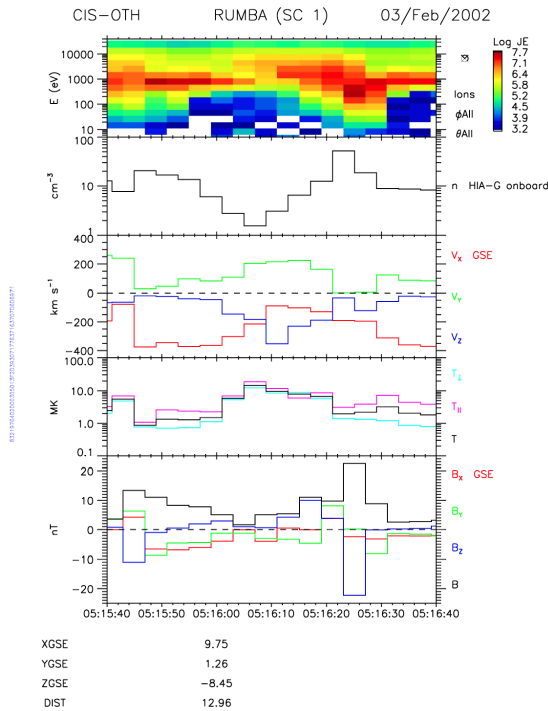


FIGURE 2. A density hole observed on 3 February 2002. From top to bottom are energy spectrogram, density, bulk speeds in GSE, temperature parallel and perpendicular to \mathbf{B} , and magnetic field and \mathbf{B} -field components.

Minimum variance analysis yields $\mathbf{k} = (-0.89, 0.43, -0.18)$ and V_{sc} , ~ 281 km/s. Noting that the solar wind speed is $V_{sw} = (-350, 70, -20)$ km s^{-1} , the phase velocity in the plasma rest frame in the direction \mathbf{k} is $V_{pl} = V_{sc} - \mathbf{k} \cdot \langle \mathbf{V} \rangle = -62$ km s^{-1} . The wave is propagating sunward with a speed ~ 62 km/s but is convected earthward with the solar wind. The plasma frame velocity is approximately the Alfvén speed, ~ 47 km s^{-1} of the ambient solar wind, where we used $B \sim 8.3$ nT and solar wind density of $n \sim 15$ cc^{-1} . The angle between \mathbf{k} and the \mathbf{B} -field is $\sim 60^\circ$ - 68° . The wave is thus an obliquely propagating wave.

Knowing \mathbf{k} , we can project the $\delta \mathbf{B}$ and $\delta \mathbf{E}$ into the plane of the wave front. Figure 3 shows hodograms of the $\delta \mathbf{E}$ and $\delta \mathbf{B}$ components in this plane from which one sees the waves are right hand elliptically polarized in the spacecraft frame and thus they are left handed in the plasma frame. The $\delta \mathbf{E}$ -field is perpendicular to the $\delta \mathbf{B}$, indicating these are plane electromagnetic waves.

Four spacecraft timing analysis also enabled us to estimate the size of this density hole to be ~ 1800 km. This is roughly the Larmor radius of 1 keV protons in a magnetic field $B = 5 \times 10^{-9}$ T. A similar analysis was performed for the density hole in Figure 1. This event was accompanied by large amplitude high frequency variations making timing analysis more complicated. Moreover the spacecraft were separated by only a few hundred km. The rough estimate of the hole size obtained is ~ 5100 km.



FIGURE 3. Sense of polarization for magnetic (left) and electric (right) fields. The left column of each shows hodograms in the plane normal to \mathbf{k} . The second and third columns are hodograms in the other planes. Observations are shown from the four Cluster spacecraft. The asterisk indicates the start point. Both electric and magnetic fields are right hand elliptically polarized in the spacecraft frame. In the plasma frame, they are left hand elliptically polarized.

CONCLUSION

We have presented observations of current densities and low frequency electromagnetic waves associated with density holes in the upstream region of the bow shock. Our analysis shows the currents in the upstream edge are large and are associated with waves that are left hand elliptically polarized in the plasma frame. These waves are most likely to be ion cyclotron waves propagating sunward in the solar wind frame but convected earthward by the solar wind and the spacecraft

observes them as a right handed polarized wave. These waves appear to be growing nonlinearly into solitary pulses forming a shock-like structure [6]. Density holes have features similar to SLAMS. Although the exact relationship between density holes and SLAMS is to be established, a few of the SLAMS events that have been published [12, 13] are accompanied by density holes. SLAMS, like density holes, have nearly vanishing magnetic field at the center and the field is steepened 2-4 times the ambient solar wind values at the edge. The mechanisms responsible for the nonlinear growth is unknown and remains a challenge to theorists.

ACKNOWLEDGEMENT

The research at the University of California, Berkeley is performed under the auspices of a NASA grant No. NNG04GF23G. Cluster is a joint project of the European Space Agency and the National Aeronautics and Space Administration.

REFERENCES

1. G. K. Parks, E. Lee, F. Mozer, et al., *Phys. of Plasmas*, **13**, 050 701-1 (2006).
2. G. K. Parks, E. Lee, N. Lin, et al., *AIP Conference Proceedings*, **932**, 9 (2006).
3. S. Schwartz, C. Chaloner, P. Christiansen et al., *Nature*, **318**, 269 (1985).
4. M. Thomsen, J. Gosling, S. Fuselier, et al., *J. Geophys. Res.*, **91**, 2961 (1986).
5. D. Sibeck, T. Phan, R. Lin, et al., *J. Geophys. Res.*, **107**, 1271 (2002).
6. N. Lin, E. Lee, F. Mozer et al., submitted to *Anales Gephysicae*, May (2008).
7. F. Neubauer and K. -H. Glassmeier, *J. Geophys. Res.*, **95**, 19115 (1990).
8. M. Dunlop, D. Southwood, K. H. Glassmeier et al., *Adv. Space Res.*, **8**, 273 (1988).
9. U. Motschmann, T. Woodward, K. H. Glassmeier et al., *J. Geophys. Res.*, **101**, 4961 (1996).
10. G. Chanteur and F. Mottez, *ESA WPP-047*, 341 (1993)
11. F. Mottez and G. Chanteur, *J. Geophys. Res.* **99**, 13499 (1994).
12. E. Lucek et al., *Ann. Geophys.* **20**, 1699 (2002).
13. E. Lucek, T. Horbury and Balogh et al., *J. Geophys. Res.* **109**, A06207 (2004).